Memoirs of the School of Engineering, Okayama University Vol.13, February 1979

Effects of the Fluctuation of Solute Concentration in Al-Zn Alloys on the Aging at Low Temperatures; II. Electron Microscopy and Measurements of SAXS Intensity

Mutsuo OHTA*, Masuo YAMADA*, Teruto KANADANI** and Akira SAKAKIBARA*

(Received January 31, 1979)

Synopsis

The effects of the fluctuation of solute concentration on the process of aging in Al-10wt%Zn alloy were studied by measurements of the intensity of small-angle X-ray scattering and by electron microscopy. Specimen was quenched from a higher temperature(T_{Q1}, mainly 300°C) to an intermediate temperature (T_{Q2}, 110~230°C), held there for a time, quenched again into iced water and aged isothermally at 0°C or 40°C. Results obtained are as follows: (1) When the specimen was held at T_{Q2} for a sufficient time and aged at relatively high temperatue(e.g. 1hr at 125°C and aged at 40°C), a two-step increasing of both resistivity and integrated intensity was found. (2) Each of the steps has characteristics of the formation of G.P. zones by the spinodal decomposition. (3) When the maximum resistivity(ρ_{max}) takes a minimum, size distribution of the G.P. zones, estimated from the difference between Guinier and Porod radii, is much broader than that at ρ_{max} in the usual direct quenching. (4) When the holding time at T_{Q2} is long enough, the size distribution at ρ_{max} is as broad as that at ρ_{max} in the usual case. (5) After a prolonged aging under the condition that ρ_{max} takes minimum, G.P. zones grow markedly and become oblate ellipsoidal with a

* Department of Industrial Science

** Okayama University of Science

major axis of about 20nm. (6) These results are consistently understood in terms of the fluctuation of solute concentration at T_{Q2} and the change in the concentration of vacancies during annealing at T_{Q2}. That is, it is considered that these results are due to the difference in aging behavior between the regions of relatively high concentration and the ones of low concentration induced by the fluctuation.

1. Introduction

Effects of the fluctuation of solute concentration on the low-temperature aging have been found in Al-Zn alloys by measurements of the electrical resistivity (1). When an alloy was quenched from a higher temperature to an intermediate temperature, held there for a time, quenched again into iced water and aged isothermally, maximum resistivity of the aging curve varied with the holding time at an intermediate temperature. This variation was pointed out to be mainly due to the fluctuation of solute concentration and the vacancy concentration. Experiments of small-angle X-ray scattering(SAXS) and transmission electron microscopy(TEM) have been carried out with Al-10wt%Zn alloy to investigate further the effects of the fluctuation on the formation of G.P. zones.

2. Experimental Procedures

An alloy of Al-10wt%Zn was prepared in the same method with those for the resistivity measurements (1). Specimens for X-ray measurements, ca. 50x10mm^2, were cut off from cold-rolled strips of 0.1mm thick and electro-polished in ethanol perchrolic-acid solution. Isothermal aging curves were examined by measurements of electrical resistivity also for these specimens, where leads of the alloy of the same composition were spot-welded to the specimen after electro-polishing. Thin films for electron microscopy were prepared by electro-polishing the strips of 0.1mm thick after appropriate heat treatments. Two-step quenching was done as in the resistivity mesurements (1).

Intensity of SAXS was measured photographically. In order to take a photograph of weak scattering from the specimen aged to a certain stage, measurements were carried out as follows. $CuK\alpha_1$ radiation monochromatized by a bent quartz crystal was used. In order to avoid

the effect of scattered X-ray by air, path of the X-ray from just after the monochromator to the X-ray film was evacuated, so the specimen and the film were in vacuo. The specimen was attached to the bottom of the Dewar vessel fitted on the cover of the vacuum chamber. Scattering from air was thus eliminated perfectly and frost on the specimen could be avoided, so an exposure for several hundred hours was facilitated. A specimen at a certain aging stage, the stage being checked by resistivity measurements, was attached quickly and carried in the camera, blowing cold dry nitrogen gas to the specimen. These treatments prevented the frosting and the rising of temperature. Thickness of the specimen was measured every time after exposure with micrometer. Scattering intensity was obtained by measuring the blackness on the film with microphotometer. The blackness of the reference lines, which were photographed at a corner of the film by changing the exposure time, was used as a standard (2). When the reference lines were photographed, the film was located between the focus of the convergent flux and the monochromator in order to reduce the error originated from the grain size of the emulsion on the film. Relative intensity of scattering on each film was calculated by obtaining the amount of the incident beam in which the contribution of $\lambda(\mathrm{Cuk}\alpha_1)/3$ and $\lambda(\mathrm{Cuk}\alpha_1)/4$ was subtracted.

Preparation of the specimen, setting and observation were done near the room temperature for the electron microscopy, so the change of the state in the alloy during these operation could not be avoided. Hence, only the specimen aged for a long time was examined. HU-200E type electron microscope was used and operated at 100 or 200kV.

3. Results

In Figs. 1 and 2 isothermal aging curves of the X-ray specimen of the Al-10wt%Zn alloy by measurements of resistivity are shown when T_{Q1}=300°C, T_{Q2}=125°C, holding time at T_{Q2} was varied in the manner shown in the figure and T_A=40°C or 0°C after quenching into iced water. SAXS intensity was measured at the stage indicated by arrows in the figures. These aging curves are similar to those of the specimen prepared properly for resistivity measurements in the shapes, but differ from them in the aging rate which is slower in these curves. Plots of ρ_{max} vs. $t(T_{Q2})$ are shown in Fig.3 for these curves together with those of the resistivity specimen. The time $t(T_{Q2})$ corresponding to the minimum of ρ_{max} is shorter than that of the resistivity specimen.

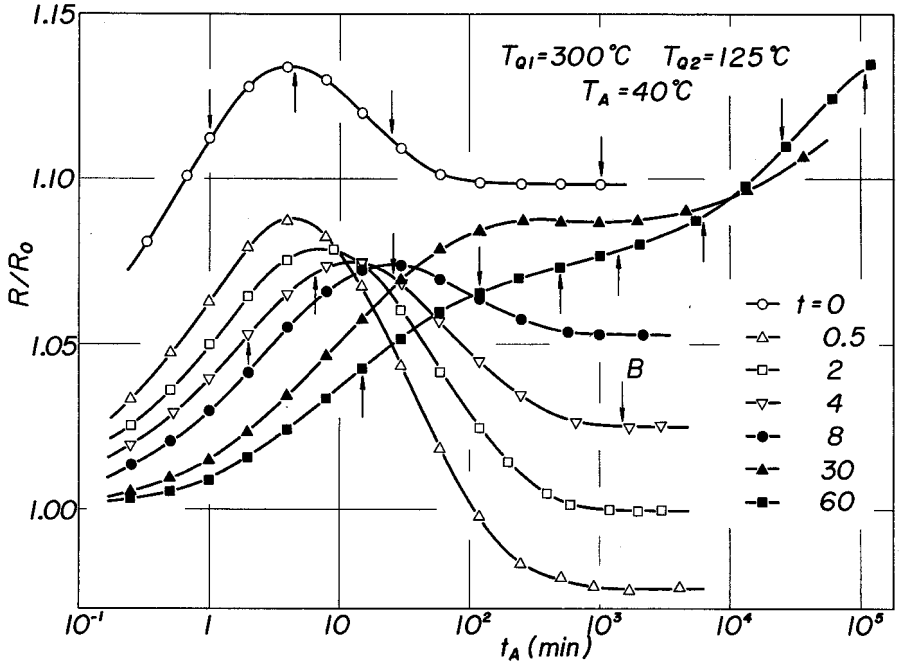

Fig.1 Isothermal aging curves of the specimen for X-ray experiments (T_A=40°C). Held for t min at T_{Q2}=125°C. SAXS was examined at the stages indicated by arrows.

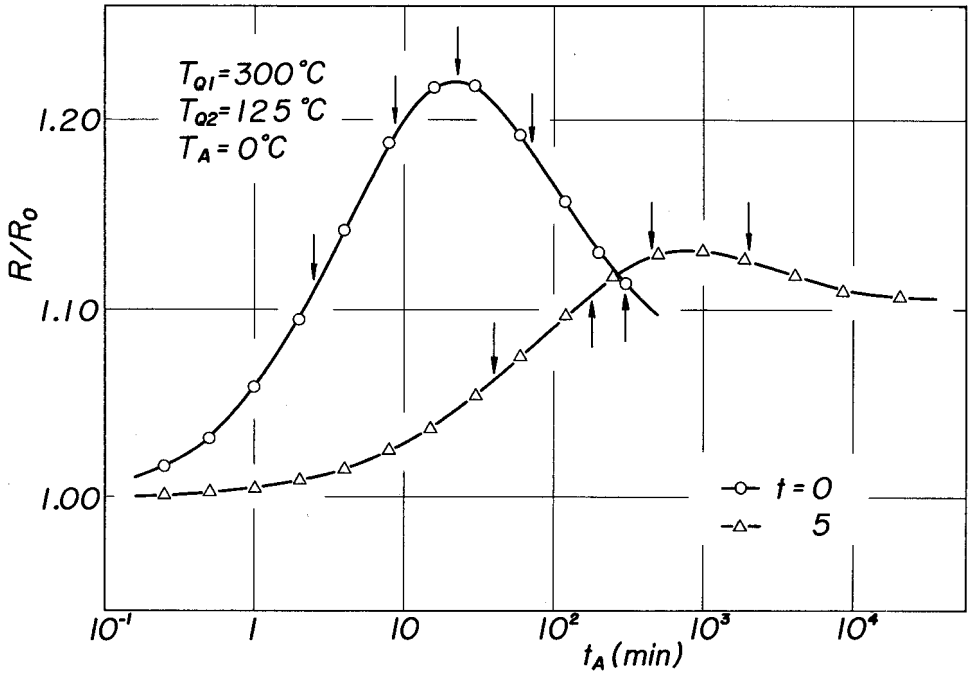

Fig.2 Isothermal aging curves of the specimen for X-ray experiments (T_A=0°C). Held for t min at T_{Q2}=125°C. SAXS was examined at the stages indicated by arrows.

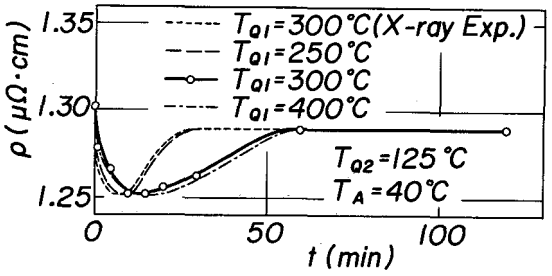

Fig.3 ρ_{max} vs. holding-time at T_{Q2} (from Fig.1). Together with those of the specimen prepared properly for resistivity measurements quenched from various T_{Q1} to T_{Q2}=125°C (1).

In Fig.4 profiles of SAXS intensity are shown for the specimen aged at the stage indicated by the arrows in Fig.1, where T_{Q1}= 300°C, T_{Q2}=125°C, t(T_{Q2})=60min and T_A=40°C. Dashed line, I_{Laue}, is a calculated intensity of Laue scattering. The relative position at higher angle of the curves with various treatments and that of I_{Laue} is reasonable. For instance Laue scattering from the matrix solid-solution, when the specimen has been aged at 40°C after quenching from 300°C into iced water and has reached at the stage of the maximum resistivity, corresponds almost to the back-ground scattering; the solute concentration in the matrix calculated from the back-ground intensity is 2.9%, near 2.6±1.5% previously reported (3). The precision of the intensity measurement, therefore, may be considerable.

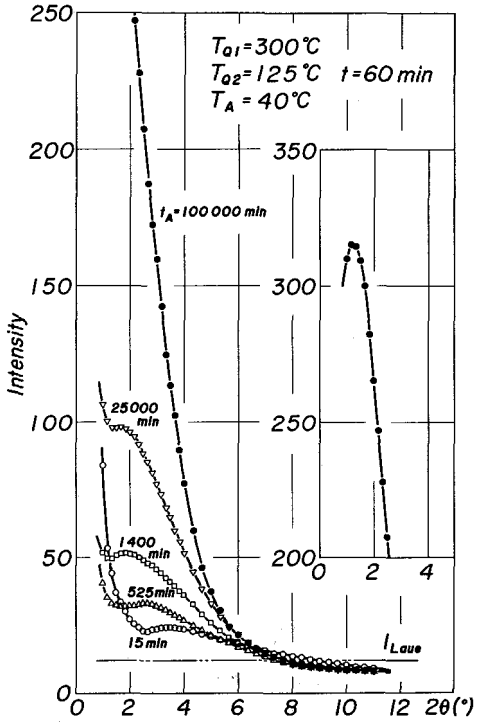

Fig.4 SAXS profiles. Held for 60min at 125°C and aged at 40°C(Fig.1).

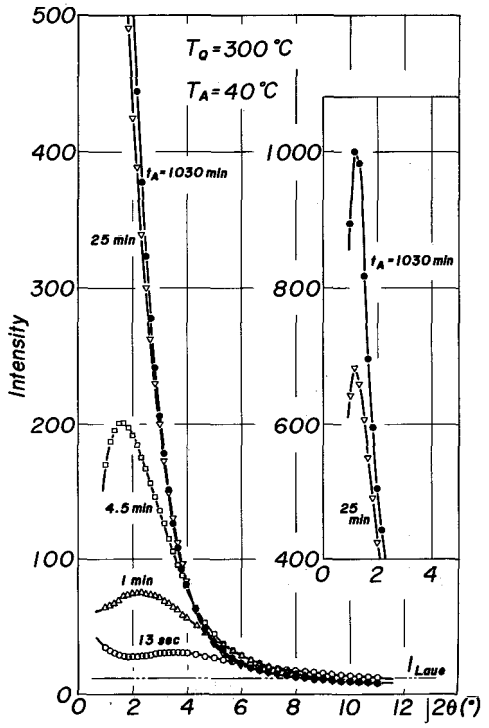

Fig.5 SAXS profiles. Directly quenched and aged at 40°C(Fig.1).

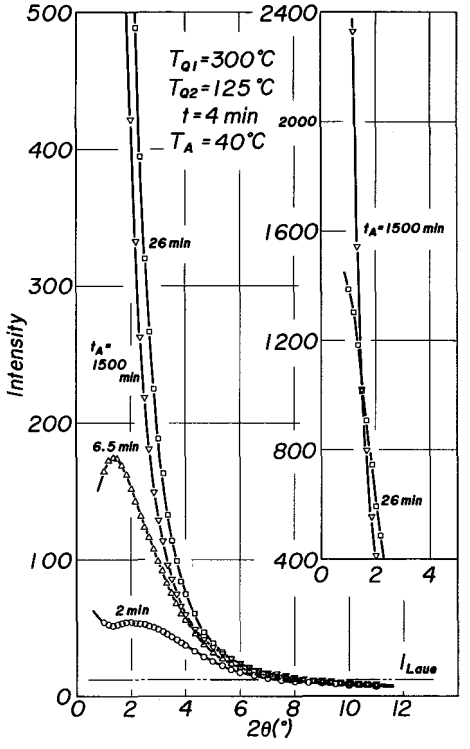

Fig.6 SAXS profiles. Held for 4min at 125°C and aged at 40°C(Fig.1).

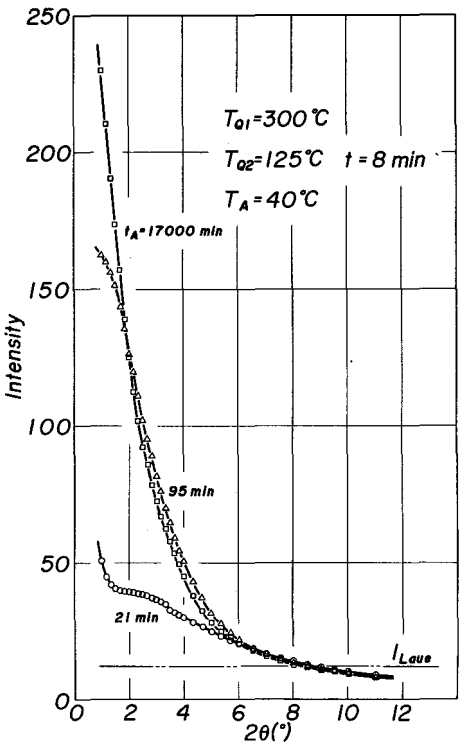

Fig.7 SAXS profiles. Held for 8min at 125°C and aged at 40°C(Fig.1).

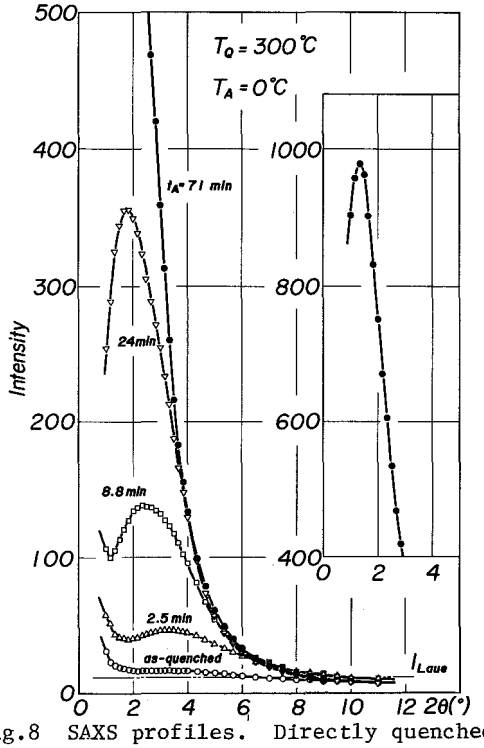

Fig.8 SAXS profiles. Directly quenched and aged at 0°C(Fig.2).

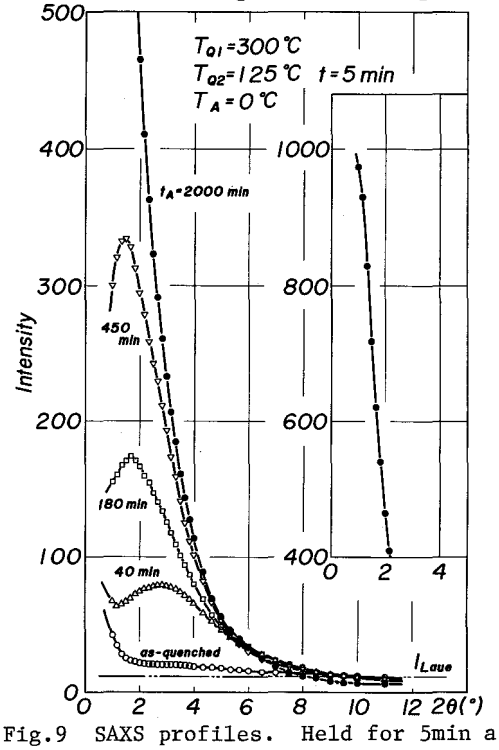

Fig.9 SAXS profiles. Held for 5min at 125°C and aged at 0°C(Fig.2).

The scattering profiles in the figure are similar in shape to those from G.P. zones formed during a usual aging treatment; they take a maximum at 2θ~1° and decrease with decreasing scattering angle. The shape of the profile is not varied even when the aging curve by resistivity measurements varies and has two stages of increasing.

In Figs. 5~7, SAXS profiles are shown for the specimens after the heat treatments indicated by arrows in Fig.1. In Figs. 8 and 9, SAXS profiles for the specimens relevant to Fig.2 are shown.

To examine whether the profiles obey Porod's law or not, s^4I is plotted against s^4, where I is the scattering intensity and s the scattering vector. Cross section of the incident beam was 3.3x0.1 mm^2 on the film where the intensity along the height was homogeneous, and the specimen-film distance was about 100mm. When the scattering intensity was desmeared (4,5), it increased only a little at higher angle, so the row data are used in the plots.

In Fig.10 s^4I vs. s^4 plots are shown in the case where T_{Q1}=300°C, T_{Q2}=125°C, T_A=40°C. For the case of direct quenching from 300°C into iced water, Porod's law is obeyed after a relatively short aging time(Fig.10a), i.e., soon after the resistivity passes the maximum. However, as shown in

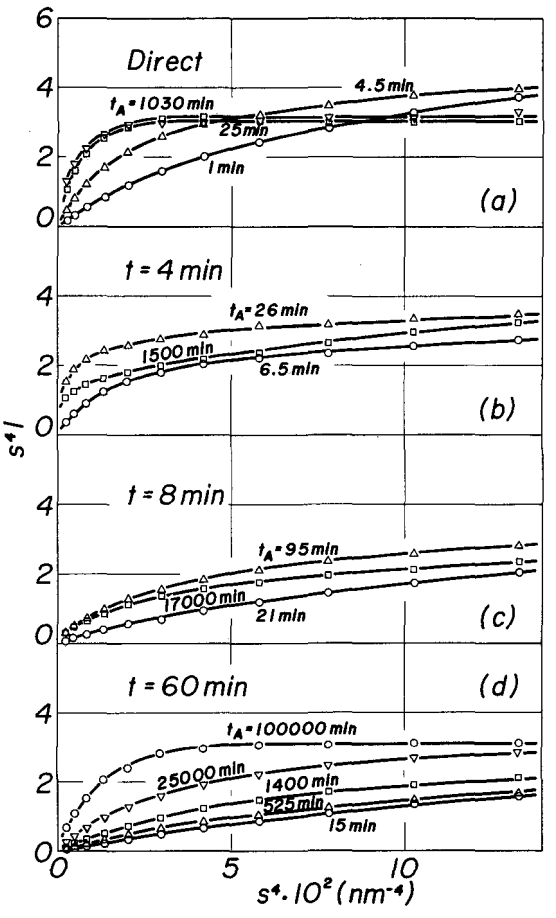

Fig.10 s^4I vs. s^4 plots. T_A=40°C.

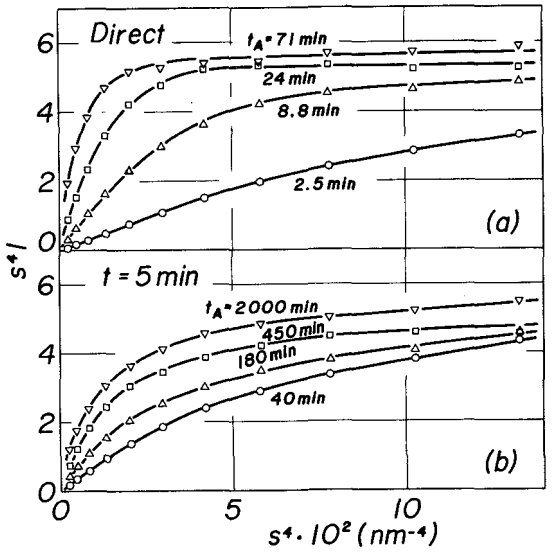

Fig.11 s^4I vs. s^4 plots. T_A=0°C.

Fig.10b, Porod's law is not obeyed for the case that the specimen was held for 4min at T_{Q2}, even when the resistivity reached the stationary value after passing the maximum, i.e., at the stage indicated by an arrow marked with B in Fig.1. On the other hand, in the case where $t(T_{Q2})$=60min, Porod's law is obeyed when the resistivity reaches maximum, though aging time then was very long, 10^5min.

In Fig.11 s^4I vs. s^4 plots are shown as in Fig.10, but when T_A= 0°C. In this case also, for the specimen aged after quenching directly, Porod's law is obeyed at the stage of ρ_{max}, while for the specimen held at T_{Q2} for 5min before quenching into iced water, Porod's law is not obeyed even after the aging fourfold longer than the time in which resistivity reaches maximum.

Table 1 Guinier and Porod radii and integrated intensities for various heat treatments.

Specimen			R_G (nm)	R_P (nm)	Q_0
T_A (°C)	$t(T_{Q2})$ (min)	t_A(min)			
0	0	2.5	0.57	-	0.13
		8.8	0.83	-	0.15
		24(ρ_{max})	1.01	0.50	0.22
		71	1.22	0.62	0.30
	5	40	0.68	-	0.16
		180	0.81	-	0.18
		450(ρ_{max})	0.96	-	0.19
		2000	1.73	-	0.21
40	0	1	0.67	-	0.12
		4.5(ρ_{max})	0.90	-	0.16
		25	1.43	0.62	0.17
		1030	1.86	0.68	0.19
	4	6.5	0.95	-	0.17
		26(ρ_{max})	1.81	-	0.20
		1500	3.10	-	0.21
	60	15	0.48	-	0.08
		120	0.62	-	0.07
		525	0.62	-	0.06
		1400	0.69	-	0.09
		6300	0.78	-	0.12
		25000	0.81	-	0.09
		100000(ρ_{max})	1.07	0.58	0.14

Values of Guinier radius R_G, Porod radius R_P and integrated intensity Q_0 were obtained from SAXS intensity for each aging stage and summerized in Table 1. Porod radius cannot be obtained when Porod's law is not obeyed, and it may be considered that there are many G.P. zones of which the size is not so large as to obey Porod's law. Following facts could be summerized from this table:

(a) In the case of direct quenching from 300°C into iced water, Porod's law is obeyed when R_G exceeds 1.0nm for both 40 and 0°C aging.

(b) In the case that the holding time at 125°C is short and corresponds to the minimum of the ρ_{max}-$t(T_{Q2})$ plot, Porod's law is not yet obeyed when R_G exceeds 1.5nm. The law is not obeyed even when R_G reaches 3.1nm for the specimen of $t(T_{Q2})$=4min and 40°C aging.

(c) In the case that the holding time at 125°C is 60min and T_A=40°C, Porod's law is obeyed when R_G exceeds 1.0nm and resistivity reaches maximum.

(d) Difference between R_G and R_P may be considered as a measure of the breadth of the distribution of the sizes of G.P. zones. When Porod's law is not obeyed, it is assumed that an average radius corresponding to R_P is smaller than that obtained when the law is obeyed. The distribution of sizes thus obtained is broad when $t(T_{Q2})$ is short and is not so broad when $t(T_{Q2})$ is long as that in the case of direct quenching.

(e) Integrated intensity for the specimen held at 125°C for 4min and aged at 40°C is larger at the later stage of aging than that for the specimen directly quenched. R_G then is larger than the other.

(f) In the case where t(125°C)=60min, integrated intensity increases at first, remains constant from 15min to 1.4×10^3min of aging and increases thereafter, which accords with the variation of resistivity.

In Photo. 1 transmission electron micrographs of the specimen aged at 0°C are shown when T_{Q1}=300°C, T_{Q2}=110°C and the holding time at T_{Q2} is 0, 5, 30min. The temperature 110°C is the highest one where formation of G.P. zones by the nucleation-and-growth mechanism is recognized, but G.P. zones may not be formed in the present experiment because of the short holding time at the temperature. The holding time at 110°C corresponding to the minimum of ρ_{max} may be shorter for this specimen than 10min obtained from Fig.7 of the preceding report (1), perhaps 5min or so, because the thickness of this specimen during the heat treatment is still thinner than the one for X-ray measurements. Then, holding for 30min at 110°C is sufficient for the specimen to be brought to the stationary stage in the

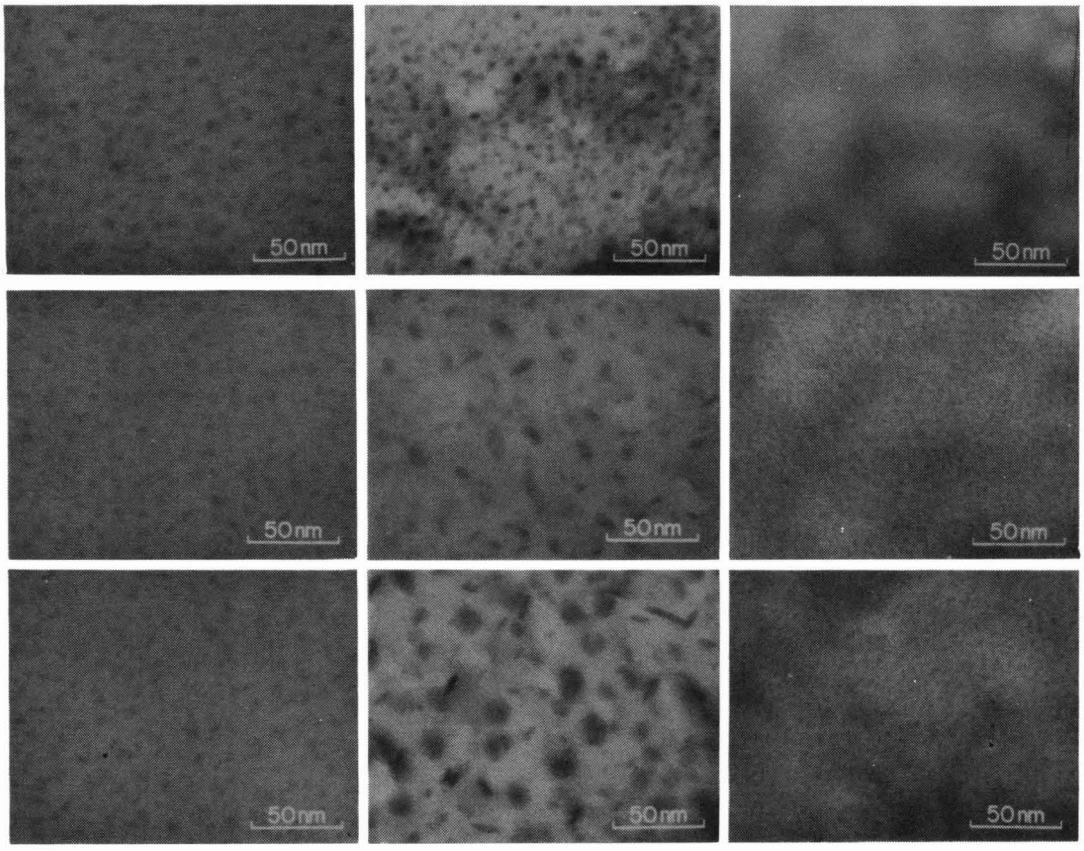

(a) (b) (c)

Photo.1 Transmission electron micrographs of the specimens aged at 0°C for 1000(top), 4000(center), 30000min(bottom). T_{Q2}=110°C. (a) directly quenched, (b) $t(T_{Q2})$=5min, (c) $t(T_{Q2})$=30min.

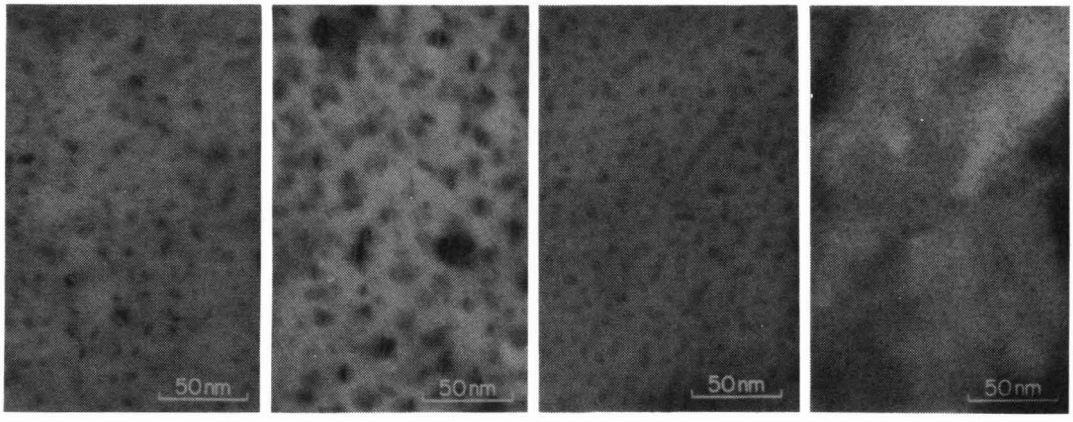

(a) (b) (c) (d)

Photo.2 TEM of the specimens aged at 0°C for 10^6min. T_{Q2}=130°C. (a) directly quenched, (b) $t(T_{Q2})$=30sec, (c) $t(T_{Q2})$=5min, (d) $t(T_{Q2})$=20min.

ρ_{max}-$t(T_{Q2})$ curve. It is observed in Photo.1 that G.P. zones grow more rapidly and become oblate ellipsoidal relatively early in the aging process in the specimen held for a short time at 110°C than in the specimen directly quenched or the specimen held longer at 110°C. Sizes of these zones are the same in the whole crystal except near the grain boundary and they are homogeneously distributed. In Photo. 2 similar results are shown also when T_{Q2}=130°C.

4. Discussions

It may be considered from the similar behavior of the aging curves that the fluctuation of solute concentration has the same effects on the aging process in the specimen for X-ray measurements and the one for resistivity measurements. Slower aging rate in the former specimen is probably due to the thickness which is a fourth of the latter. Though the maximum cooling rate during quenching may be larger, cooling before emerging into iced water may be large for a thin specimen and so the effective quenching temperature may be lowered. Moreover, migration of excess vacancies to the surface may occur more during the rather slow cooling from 0°C to liquid nitrogen temperature. Effectively lowered vacancy concentration is also found in the ρ_{max}-$t(T_{Q2})$ curves(Fig.3), where the curve for a thinner specimen quenched from 300°C corresponds to the one for a quenching temperature lower than 250°C.

It is well known that G.P. zones are formed by the spinodal mechanism below the spinodal temperature. Above that temperature formation of G.P. zones by the nucleation-and-growth mechanism was reported (6~8). According to these reports, resistivity does not increase during aging and SAXS intensity does not take maximum, i.e., decreases monotonically with increasing scattering angle, when G.P. zones are formed by the nucleation-and-growth mechanism. On the other hand, when G.P. zones are formed by the spinodal decomposition, aging curves by resistivity measurement show a maximum and a hallow pattern is observed on the SAXS photograph. In the present results, when T_{Q1}= 300°C, T_{Q2}=125°C, $t(T_{Q2})$=60min and T_A=40°C, resistivity increases with two stages as in Fig.1. Integrated intensity of SAXS also varies with two stages for this heat treatment as shown in Table 1. Moreover, SAXS profiles in both stages have the maximum of intensity, therefore, it is considered that both stages in the aging curve have the characteristics of the spinodal decomposition. Appearance of two stages in the aging may be due to the two spinodal decompositions which occur in defferent rates.

To discuss the effects of the fluctuation on the formation of G.P. zones further, it is assumed that there should be regions of high solute concentration(C regions) and the ones of low concentation(D regions) being caused by fluctuation in the alloys, and that G.P. zones are formed by the spinodal decomposition in both regions at the aging temperature. Based upon this assumption, present experimental results may be explained by the differences of the rate of formation and growth of the G.P. zones and the limit of sizes to which G.P. zones can grow in an ordinary aging time in C and D regions. If details of the aging behaviors were known for the alloy of homogeneous distribution of solute atoms corresponding to either of the C and D regions when the vacancy concentration was as low as in the present cases, obtained results might be explained in a semi-quantitative manner. However, a homogeneous solid solution with a concentration around 10wt%Zn which contains equilibrium vacancies at T_{Q2} cannot be realized by heat treatments because of the occurance of fluctuation. Therefore, the aging behaviors of the alloys of various solute concentration with much higher vacancy concentration than that in the present alloys must be refered.

Such results hitherto obtained (3,9) are summerized as follows:

(i) The ratio of the time to reach ρ_{max} in the isothermal aging curve of a higher Zn concentration to the one of a lower concentration is always smaller than 1, i.e., aging rate is larger in the alloys of higher concentration. When T_A is low (eg. less than 20°C for 10%Zn alloy), the ratio does not vary with temperature, but in a higher temperature region it decreases with increasing T_A, i.e., difference in the aging rate becomes large.

(ii) The value of the stationary resistivity(ρ_E) observed after ρ_{max} in the aging curve depends on the quenching temperature T_Q. When T_Q's are lower than 350°C, it becomes larger as T_Q becomes low and Guinier radius of the zones becomes small as ρ_E becomes large, that is to say, as the vacancy concentration decreases, aging proceeds less far, G.P. zones stop growing at small sizes and ρ_E remains large. This tendency is more significant when the aging temperature is high.

Based on these results, interpretation of the present experimental results will be attempted.

(A) The case of minimum ρ_{max} ——— $t(T_{Q2})$ being short

Vacancy concentration is higher than the equilibrium one at T_{Q2}. Due to the difference in the aging rate, G.P. zones in C regions must be large but those in D regions remain still small when the resistivity reaches maximum during aging. Porod's law is not obeyed even when

R_G becomes larger, as is shown at the corresponding row in Table 1, because of the existence of small zones in D regions. In this case, Ostwald ripening may proceed easily when the specimen is aged further, since there are G.P. zones with very different sizes in the alloy. This agrees well with the result of (b) in Photo.1 or (c) in Photo.2.

When the value R_G of the specimen held at T_{Q2} for 4min and aged at 40°C is compared with that of the specimen held for 5min and aged at 0°C, the former is much larger than the latter. This is well understood by (i) above, that is, G.P. zones in C regions grow more rapidly than in D regions at a higher aging temperature.

(B) The case of long holding at T_{Q2}

Vacancy concentration must be very low and nearly equal to the equilibrium value at T_{Q2}. Therefore, G.P. zones cannot grow so large even in C regions and the value ρ_E remains high. The rate of growth of the zones in D regions is still slower but Ostwald ripening does not occur until after a long aging time, because G.P. zones in C regions canot be so large. Since G.P. zones in C regions remain small, Porod's law may be obeyed at a rather small R_G, as in the case shown in Table 1 on the specimen which was aged for 10^5min at 40°C after $t(T_{Q2})$=60min. Surpressing of Ostwald ripening is also recognized with TEM observation; G.P. zones are small as shown in Photo.1(c) and 2(d).

In this case the aging curve at 40°C shows two-step aging but the one at 0°C does not. It is considered to be probable that the rate of aging in C and D regions does not differ each other so much when T_A=0°C.

The authors are grateful to Professor T. Ino, Faculty of Science of Osaka City University, for help with the photometry.

References

(1) M. Ohta, T. Kanadani, M. Yamada and A. Sakakibara: Memoirs School Eng., Okayama Univ., 13(1979), 95.

(2) M. Ohta: J. Japan Inst. Metals, 27(1963), 140(in Japanese).

(3) M. Ohta, F. Hashimoto and H. Maeda: J. Japan Inst. Metals, 32 (1968), 1097(in Japanese).

(4) O. Kratky, G. Porod and L. Kahovec: Z. Electrochem., 55(1951). 53.

(5) A. Guinier and G. Fournet: Small-Angle Scattering of X-Rays,

John Wiley & Sons, New York(1955), 118.

(6) A. Junqua, J. Mimault, J. Delafond and J. Grilhe: Scripta Met., 8(1974), 317.

(7) J. Allain, A. Naudon, J. Delafond, A. Junqua and J. Mimault: Scripta Met., 8(1974), 831.

(8) J. Delafond, A. Junqua, J. Mimault and J. P. Riviere: Acta Met., 23(1975), 405.

(9) M. Ohta and F. Hashimoto: J. Japan Inst. Metals, 36(1972), 321 (in Japanese).